PHYSICAL REVIEW C **84**, 011901(R) (2011)

Elliptic flow in Pb+Pb collisions at $\sqrt{s_{NN}} = 2.76$ TeV: Hybrid model assessment of the first data

Tetsufumi Hirano,[1,2,*] Pasi Huovinen,[3,†] and Yasushi Nara[4,‡]

[1]*Department of Physics, The University of Tokyo, Tokyo 113-0033, Japan*

[2]*Nuclear Science Division, Lawrence Berkeley National Laboratory, Berkeley, California 94720, USA*

[3]*Institut für Theoretische Physik, Johann Wolfgang Goethe-Universität, D-60438 Frankfurt am Main, Germany*

[4]*Akita International University, Yuwa, Akita-city 010-1292, Japan*

(Received 20 December 2010; published 7 July 2011)

We analyze the elliptic flow parameter v_2 in Pb+Pb collisions at $\sqrt{s_{NN}} = 2.76$ TeV and in Au+Au collisions at $\sqrt{s_{NN}} = 200$ GeV using a hybrid model in which the evolution of the quark gluon plasma is described by ideal hydrodynamics with a state-of-the-art lattice QCD equation of state, and the subsequent hadronic stage by a hadron cascade model. For initial conditions, we employ Monte Carlo versions of the Glauber and the Kharzeev-Levin-Nardi models and compare results with each other. We demonstrate that the differential elliptic flow $v_2(p_T)$ hardly changes when the collision energy increases, whereas the integrated v_2 increases due to the enhancement of mean transverse momentum. The amount of increase of both v_2 and mean p_T depends significantly on the model of initialization.

DOI: 10.1103/PhysRevC.84.011901 PACS number(s): 25.75.Nq, 12.38.Mh, 12.38.Qk

The recently started heavy-ion program at Large Hadron Collider (LHC) in CERN opens up opportunities to explore the deconfined matter, the quark gluon plasma (QGP), in a wider temperature region. Elliptic flow [1], which played an essential role to establish the new paradigm of the strongly coupled QGP [2,3] at Relativistic Heavy-Ion Collider (RHIC) in Brookhaven National Laboratory (BNL) [4], is one of the key observables at LHC to investigate the bulk and transport properties of the QGP. First elliptic flow data in Pb+Pb collisions at $\sqrt{s_{NN}} =$ 2.76 TeV were recently published by the ALICE Collaboration [5]. The first goal of flow measurements is to see whether hydrodynamic models reproduce the flow as well at LHC as at RHIC, and thus whether the QGP depicts similar strong coupling nature at LHC.

This Rapid Communication is a sequel to our previous work [6] where we predicted the elliptic flow parameter v_2 before any LHC data was available. In this publication we take the advantage of the first LHC data [5,7] to fix the final particle multiplicity, which removes the main uncertainty in our prediction, and allows us to use a Glauber type initialization too. We calculate the elliptic flow parameter v_2 and its transverse momentum (p_T) dependence in Pb+Pb collisions at LHC and compare them with the data. Our model for the space-time evolution of the matter is the same we used in Ref. [6]: A hybrid model where the expansion of the QGP is described by ideal hydrodynamics [8], and the subsequent evolution of hadronic matter below switching temperature $T_{\rm sw} = 155$ MeV, is described using a hadronic cascade model JAM [9]. During the fluid dynamical stage, we employ EoS $s95p$-v1.1, which interpolates between hadron resonance gas at low temperatures and recent lattice QCD results by the hotQCD collaboration [10,11] at high temperatures in the same way as $s95p$-v1 [12], but the hadron resonance gas part contains the same hadrons and resonances as the JAM hadron cascade [9]. The details of the interpolating procedure are explained in Ref. [12] and the parametrization and EoS tables are available at Ref. [13].

Initial time of hydrodynamic simulations is fixed to be $\tau_0 =$ 0.6 fm/c throughout this work. For initial conditions in the longitudinal direction, we assume the Bjorken scaling solution [14]. To initialize the density distributions in the transverse plane, we utilize two Monte Carlo approaches: Monte Carlo–Glauber (MC-Glauber) model [15] and Monte Carlo–Kharzeev-Levin-Nardi (MC-KLN) model [16]. Using these Monte Carlo models, we calculated initial conditions for hydrodynamic simulations in the transverse plane with respect to the *participant plane* in our previous work [6]. These initial density profiles contain effects of eccentricity fluctuation on average. However, the ALICE Collaboration mainly obtained v_2 using the four-particle cumulant method $v_2\{4\}$ [17]. If the event-by-event distribution of eccentricity in the reaction plane is a two-dimensional Gaussian, and if v_2 is proportional to the participant eccentricity, then $v_2\{4\}$ yields the value of v_2 in the reaction plane [18,19]. Therefore we calculate in this Rapid Communication initial profiles with respect to the *reaction plane*: We average over many events using Monte Carlo calculations instead of shifting and rotating a distribution event by event to match the main and subaxes of the ellipsoids as was done in the previous work [6,20]. It should be noted that the distributions obtained in this way are not identical to the ones from the optical Glauber model or the factorized KLN (fKLN) model [21] because of finite nucleon size effects [16,22]: The collision points in the transverse plane are smeared using an inelastic cross section of $p + p$ collisions in the "mean-field" option in the Monte Carlo approach [16] to obtain smooth initial conditions for hydrodynamic simulations.

In the MC-KLN model, we calculate distribution of gluons at each transverse grid using the k_t-factorized formula [23]. Using the thickness function T_A, we parametrize the saturation

*hirano@phys.s.u-tokyo.ac.jp
†huovinen@th.physik.uni-frankfurt.de
‡nara@aiu.ac.jp

scale for a nucleus A as

$$Q_{s,A}^2(x;\boldsymbol{x}_\perp) = 2\ \mathrm{GeV}^2 \frac{T_A(\boldsymbol{x}_\perp)}{1.53\ \mathrm{fm}^{-2}} \left(\frac{0.01}{x}\right)^\lambda, \qquad (1)$$

and similarly for a nucleus B. We choose $\lambda = 0.28$ and a proportionality constant in the unintegrated gluon distribution in the k_t-factorized formula to reproduce centrality dependence of p_T spectra obtained by the PHENIX Collaboration [24]. As a default parameter set at LHC, we use the same parameters except for colliding energy and mass number of incident nuclei. This predicted $dN_{\mathrm{ch}}/d\eta \sim 1600$ at 5% most central collisions [6], which turns out to be consistent with the recent ALICE measurement [7,25].

In the MC-Glauber model, one calculates the number distributions of participants ρ_{part} and of binary collisions ρ_{coll} for a given nuclear density distribution. We model the initial entropy distribution in hydrodynamic simulations as a linear combination of ρ_{part} and ρ_{coll} in the transverse plane:

$$\frac{dS}{\tau_0 d\eta_s d^2\boldsymbol{x}_\perp} = \frac{C}{\tau_0}\left(\frac{1-\alpha}{2}\rho_{\mathrm{part}}(\boldsymbol{x}_\perp) + \alpha\rho_{\mathrm{coll}}(\boldsymbol{x}_\perp)\right). \qquad (2)$$

At the RHIC energy, the mixing parameter $\alpha = 0.18$ and the proportionality constant $C = 15.0$ in Eq. (2) are chosen to reproduce the centrality dependence of p_T spectra at RHIC [24]. We tune these two parameters in Pb+Pb collisions at LHC to reproduce the centrality dependence of charged hadron multiplicity [25]. For both initializations we do the centrality cuts according to the N_{part} distribution from the MC-Glauber model [6].

In Fig. 1, we calculate $dN_{\mathrm{ch}}/d\eta/(N_{\mathrm{part}}/2)$ as a function of N_{part} for initial conditions from the MC-Glauber and the MC-KLN models and compare them with data. The experimental data point in inelastic $p+p$ collisions at $\sqrt{s_{NN}} = 2.36$ TeV [26] is plotted at $N_{\mathrm{part}} = 2$. The MC-KLN initialization leads to remarkable agreement with the ALICE data. On the other hand, it is difficult to fit the data within the current two-component picture in the MC-Glauber model: The results from the MC-Glauber initialization with $\alpha = 0.08$ and $C = 41.4$ almost

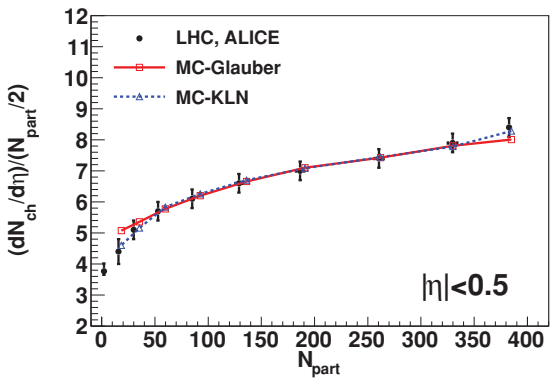

FIG. 1. (Color online) Centrality dependence of charged hadron multiplicity in the MC-Glauber and the MC-KLN initialization is compared with ALICE data [25,26]. A data point from inelastic events at $\sqrt{s_{NN}} = 2.36$ TeV in $p+p$ collisions [26] is shown at $N_{\mathrm{part}} = 2$. Each point in theoretical results from right to left corresponds to 0%–5%, 5%–10%, 10%–20%, 20%–30%, 30%–40%, 40%–50%, 50%–60%, 60%–70%, and 70% –80% centrality, respectively.

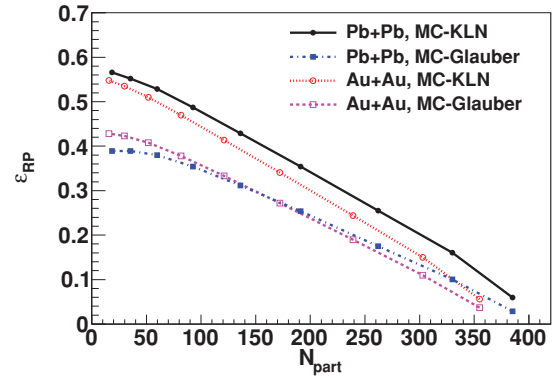

FIG. 2. (Color online) Eccentricity with respect to the reaction plane as a function of N_{part} in Pb + Pb collisions at $\sqrt{s_{NN}} = 2.76$ TeV and in Au+Au collisions at $\sqrt{s_{NN}} = 200$ GeV. Each point from right to left corresponds to 0%–5%, 5%–10%, 10%–20%, 20%–30%, 30%–40%, 40%–50%, 50%–60%, 60%–70%, and 70%–80% centrality, respectively.

trace the ones from the MC-KLN initialization and the ALICE data except for 0%–5% and 70%–80% centrality.

Shown in Fig. 2 is the initial eccentricity with respect to reaction plane as a function of N_{part} in Pb+Pb collisions at $\sqrt{s_{NN}} = 2.76$ TeV and in Au+Au collisions at $\sqrt{s_{NN}} = 200$ GeV. As previously known, the k_t-factorized formula of KLN model generates larger eccentricity than the Glauber model does [21,27]. In the MC-KLN model, eccentricity in Pb+Pb collisions at $\sqrt{s_{NN}} = 2.76$ TeV is slightly larger than that in Au+Au collisions at $\sqrt{s_{NN}} = 200$ GeV when the centrality is fixed [6]. On the other hand, in the MC-Glauber model, eccentricity in Pb+Pb collisions at $\sqrt{s_{NN}} = 2.76$ TeV is slightly smaller than that in Au+Au collisions at $\sqrt{s_{NN}} = 200$ GeV for a fixed centrality.

This is because of the smearing process we use to obtain a smooth initial profile for hydrodynamic evolution. As mentioned, we use the inelastic cross section in $p+p$ collisions, σ_{in}, to smear the distribution of collision points. This cross section is $\sim$1.5 times larger at LHC than at RHIC, and thus the smearing area, $S = \sigma_{\mathrm{in}}$ [16], is also larger at LHC, and the eccentricity is reduced. Our smearing procedure also leads to a smaller eccentricity than the conventional value of the MC-Glauber model.[1] The effect of smearing is smaller in the MC-KLN initialization, and we have checked that the eccentricity at LHC turns out to be essentially the same as at RHIC when the smearing area is the same. Systematic studies of initialization and its effects will be shown in a later publication [28].

Figure 3 shows comparison of transverse momentum distributions of charged hadrons between RHIC and LHC energies at 10%–20% and 40%–50% centralities. As clearly seen from figures, the slope of p_T spectra becomes flatter as collision energy and, consequently, pressure of produced matter increases. To quantify this, we calculate mean p_T of

[1]In the MC-Glauber model in the literature [15], one assumes δ function profile for each collision point in ρ_{part} distribution rather than a boxlike profile in the present work

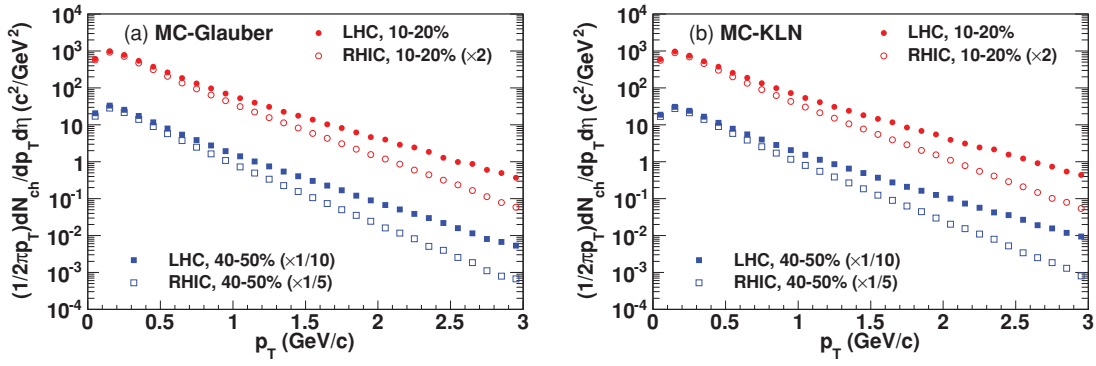

FIG. 3. (Color online) Transverse momentum distribution of charged hadrons at 10%–20% (circles) and 40%–50% (squares) centralities in Pb+Pb collisions at $\sqrt{s_{NN}} = 2.76$ TeV (solid symbols) and in Au + Au collisions at $\sqrt{s_{NN}} = 200$ GeV (open symbols). Results from (a) the MC-Glauber initialization and (b) the MC-KLN initialization. For the sake of comparison and visibility, the spectra are scaled by 2, 1/10, and 1/5 for 10%–20% at RHIC, 40%–50% at LHC, and 40%–50% at RHIC, respectively.

charged hadrons. In the MC-Glauber initialization, mean p_T increases from RHIC to LHC by 21% and 19% in 10%–20% and 40%–50% centrality, respectively. On the other hand, the corresponding fractions are 25% and 24% in the MC-KLN initialization. Because our calculations at RHIC were tuned to reproduce the p_T spectra, this means that at LHC the spectra calculated using the MC-KLN initialization are slightly flatter than those calculated using the MC-Glauber initialization.

We compare integrated v_2 for charged hadrons with respect to the reaction plane with the ALICE [5] and STAR [29] $v_2\{4\}$ data in Fig. 4. When evaluating the integrated v_2, we take account of both transverse momentum and pseudorapidity acceptance as done in the experiments (i.e., $0.2 < p_T < 5.0$ GeV/c and $|\eta| < 0.8$ for ALICE, and $0.15 < p_T < 2.0$ GeV/c and $|\eta| < 1.0$ for STAR). We want to emphasize that not only the p_T cut [30], but also the pseudorapidity cut plays an important role in a consistent comparison with the data. Because of the Jacobian for the change of variables from rapidity y to pseudorapidity η, $v_2(y = 0) < v_2(\eta = 0)$ for positive elliptic flow [31].[2] In the case of the MC-Glauber (MC-KLN) initialization in 40%–50% centrality, v_2 integrated over the whole p_T region is ∼14% (∼10%) larger at $\eta = 0$ than at $y = 0$.

When the MC-Glauber model is employed for initial profiles, centrality dependence of integrated v_2 from the hybrid approach almost agrees with both ALICE and STAR data. Because eccentricity fluctuation contributes little and negatively to $v_2\{4\}$ in non-Gaussian distribution of eccentricity fluctuation [18,19], this indicates there is only little room for the QGP viscosity in the model calculation. On the other hand, apparent discrepancy between the results from the MC-KLN initialization and the ALICE and STAR data means that viscous corrections during the hydrodynamic evolution are required.

From RHIC to LHC, the p_T-integrated $v_2(|\eta| < 0.8)$ increases by 24% and 25% in 10%–20% and 40%–50% centrality, respectively, in the MC-Glauber initialization. On the other hand, in the MC-KLN initialization, the increase reaches 42% and 44% in 10%–20% and 40%–50% centrality, respectively. Because eccentricity does not change significantly (at most ±6% in 40%–50% centrality) from RHIC to LHC as shown in Fig. 2, the significant increase of integrated v_2 must be attributed to a change in transverse dynamics.

Finally, we compare $v_2(p_T)$ of charged hadrons with ALICE [5] and STAR [29] data in 10%–20% [Fig. 5(a)] and 40%–50% [Fig. 5(b)] centrality. Interestingly, the data at LHC agree with the data at RHIC within errors. The calculated $v_2(p_T)$ shows similar independence of collision energy when MC-Glauber initialization is used, whereas MC-KLN initialization leads to a slightly larger $v_2(p_T)$ at the larger energy. For MC-Glauber results, the fit to data is fair below $p_T \sim 1.5$ GeV/c and $p_T \sim 0.8$ GeV/c momenta in the 10%–20% and 40%–50% centralities, respectively. Results from the MC-KLN initialization at both energies are significantly larger than experimental data in the whole p_T region, which again indicates necessity of viscous corrections in hydrodynamic evolution. For both initializations the difference between the data and the calculated $v_2(p_T)$ is larger in more peripheral collisions. This, too, can be understood as an indication of viscosity, because the more peripheral the collision, the smaller the system and the more anisotropic its shape, and both of these qualities enhance the dissipative effects.

Because of the relationships among the p_T spectrum, p_T averaged v_2, and p_T differential $v_2(p_T)$, the flatter the p_T spectrum, the larger the v_2 even if $v_2(p_T)$ stays the same. It is also worth noticing that the steeper the slope of $v_2(p_T)$, the larger the increase in v_2 for the same increase in mean p_T. This is the main reason why quite a similar increase of mean p_T for both MC-Glauber and MC-KLN initializations leads to a much larger increase of v_2 for MC-KLN than for MC-Glauber initialization.

At the time of this writing, the initial state of the fluid dynamical expansion of heavy-ion collisions at ultrarelativistic energies is quite uncertain. This has been a longstanding issue in the physics of heavy-ion collisions which must be by all means resolved. If color glass condensate (CGC) [32] initial conditions, like the ones obtained using the MC-KLN model

[2]Notice that even if one assumes the Bjorken scaling solution, one has to consider the pseudorapidity acceptance because $v_2(\eta)$ is not constant even if $v_2(y)$ is [31]

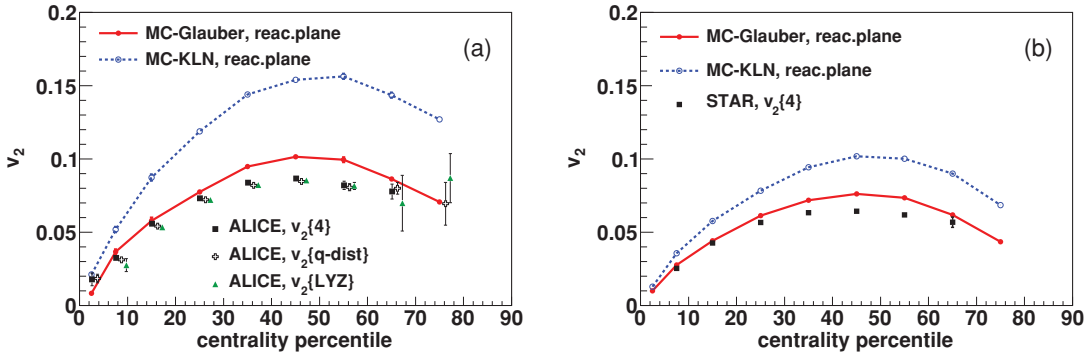

FIG. 4. (Color online) Centrality dependencies of v_2 for charged hadrons with respect to reaction plane (a) in Pb+Pb collisions at $\sqrt{s_{NN}} = 2.76$ TeV ($|\eta| < 0.8$, $0.2 < p_T < 5$ GeV/c) and (b) in Au+Au collisions at $\sqrt{s_{NN}} = 200$ GeV ($|\eta| < 1.0$, $0.15 < p_T < 2$ GeV/c) are compared with ALICE [5] and STAR [29] v_2 data, respectively. ALICE data points are shifted horizontally for visibility.

in the present work, are realized in nature at both RHIC and LHC energies, the larger deviation of v_2 from the data at LHC than at RHIC in Figs. 4 and 5 could mean that viscous effects are larger at LHC than at RHIC. This can indicate a larger specific shear viscosity, η/s, at larger temperatures. For a better interpretation of current experimental data, the issue should be clarified in the near future by determining the initial conditions better and by a more detailed analysis using a hybrid model of viscous hydrodynamics and hadron cascade [33].

In summary, we calculated transverse momentum distribution of charged hadrons, centrality dependence of integrated elliptic flow parameter v_2, and differential elliptic flow $v_2(p_T)$ in Pb+Pb collisions at $\sqrt{s_{NN}} = 2.76$ TeV and in Au+Au collisions at $\sqrt{s_{NN}} = 200$ GeV. We compared v_2 and $v_2(p_T)$ with respect to the reaction plane from the hybrid model with v_2 data mainly obtained from the four-particle cumulant method. Transverse momentum distributions become harder, whereas the shape of $v_2(p_T)$ does not change so much as the collision energy increases. Thus the increase in p_T-integrated v_2 is from the increase in mean p_T. However, the intrinsic slope of $v_2(p_T)$ depends on the initialization: The slope from the MC-KLN initialization is steeper than that from the MC-Glauber initialization, and thus essentially the same change of mean p_T leads to a larger increase of p_T-integrated v_2 for MC-KLN initialization than for MC-Glauber initialization. The larger difference between the data and our MC-KLN result at LHC than at RHIC may indicate larger dissipative effects at LHC than at RHIC. All this emphasizes the importance of understanding initial conditions in relativistic heavy-ion collisions toward extracting the bulk and transport properties of the QGP. In the future, it would be interesting to compare our results with data obtained using a more sophisticated elliptic flow analysis [19], in which both nonflow and eccentricity fluctuation effects are removed.

We thank R. Snellings for providing us with the experimental data. The work of T.H. and Y.N. was partly supported by Grant-in-Aid for Scientific Research (Grants No. 22740151 and No. 20540276, respectively). T.H. is also supported under Excellent Young Researchers Oversea Visit Program (Grant No. 21-3383) by Japan Society for the Promotion of Science. The work of P.H. is supported by the ExtreMe Matter Institute (EMMI) and BMBF (Contract No. 06FY9092). T.H. thanks X. N. Wang and H. Song for fruitful discussion, and members in the nuclear theory group at Lawrence Berkeley National Laboratory for kind hospitality during his sabbatical stay.

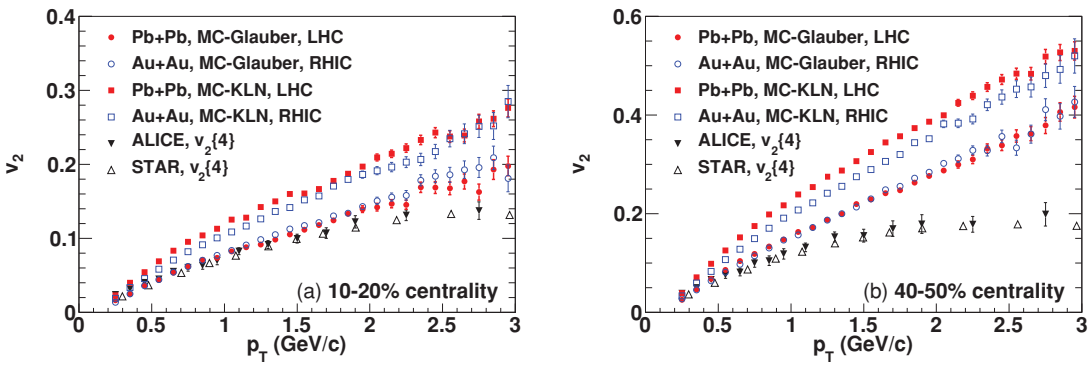

FIG. 5. (Color online) Transverse momentum dependencies of v_2 for charged hadrons in the MC-Glauber (circles) and the MC-KLN (squares) initialization are compared with ALICE [5] (triangles) and STAR [29] (band) $v_2\{4\}$ data in (a) 10%–20% centrality and (b) 40%–50% centrality. We take account of pseudorapidity cut, $|\eta| < 0.8$ (1.0), in the ALICE (STAR) data.

[1] J. Y. Ollitrault, Phys. Rev. D **46**, 229 (1992).
[2] M. Gyulassy, arXiv:nucl-th/0403032.
[3] T. D. Lee, Nucl. Phys. A **750**, 1 (2005); M. Gyulassy and L. McLerran, *ibid.* **750**, 30 (2005); E. V. Shuryak, *ibid.* **750**, 64 (2005).
[4] [http://www.bnl.gov/bnlweb/pubaf/pr/PR_display.asp?prID=05-38].
[5] K. Aamodt *et al.* (The ALICE Collaboration), arXiv:1011.3914 [nucl-ex].
[6] T. Hirano, P. Huovinen, and Y. Nara, Phys. Rev. C **83**, 021902 (2011).
[7] K. Aamodt *et al.* (The ALICE Collaboration), Phys. Rev. Lett. **105**, 252301 (2010).
[8] T. Hirano, Phys. Rev. C **65**, 011901 (2001); T. Hirano and K. Tsuda, *ibid.* **66**, 054905 (2002).
[9] Y. Nara, N. Otuka, A. Ohnishi, K. Niita, and S. Chiba, Phys. Rev. C **61**, 024901 (1999) [http://quark.phy.bnl.gov/∼ynara/jam/].
[10] M. Cheng *et al.*, Phys. Rev. D **77**, 014511 (2008).
[11] A. Bazavov *et al.*, Phys. Rev. D **80**, 014504 (2009).
[12] P. Huovinen and P. Petreczky, Nucl. Phys. A **837**, 26 (2010).
[13] [https://wiki.bnl.gov/hhic/index.php/Lattice_calculatons_of_Equation_of_State] and [https://wiki.bnl.gov/TECHQM/index.php/QCD_Equation_of_State].
[14] J. D. Bjorken, Phys. Rev. D **27**, 140 (1983).
[15] M. L. Miller, K. Reygers, S. J. Sanders, and P. Steinberg, Ann. Rev. Nucl. Part. Sci. **57**, 205 (2007).
[16] H. J. Drescher and Y. Nara, Phys. Rev. C **75**, 034905 (2007); **76**, 041903(R) (2007); [http://www.aiu.ac.jp/∼ynara/mckln/].
[17] N. Borghini, P. M. Dinh, and J. Y. Ollitrault, Phys. Rev. C **63**, 054906 (2001); **64**, 054901 (2001).
[18] S. A. Voloshin, A. M. Poskanzer, A. Tang, and G. Wang, Phys. Lett. B **659**, 537 (2008).
[19] J. Y. Ollitrault, A. M. Poskanzer, and S. A. Voloshin, Phys. Rev. C **80**, 014904 (2009).
[20] T. Hirano and Y. Nara, Phys. Rev. C **79**, 064904 (2009).
[21] A. Adil, H. J. Drescher, A. Dumitru, A. Hayashigaki, and Y. Nara, Phys. Rev. C **74**, 044905 (2006).
[22] P. Sorensen, B. Bolliet, A. Mocsy, Y. Pandit, and N. Pruthi, arXiv:1102.1403 [nucl-th].
[23] D. Kharzeev and M. Nardi, Phys. Lett. B **507**, 121 (2001); D. Kharzeev and E. Levin, *ibid.* **523**, 79 (2001); D. Kharzeev, E. Levin, and M. Nardi, Phys. Rev. C **71**, 054903 (2005); Nucl. Phys. A **730**, 448 (2004).
[24] S. S. Adler *et al.* (PHENIX Collaboration), Phys. Rev. C **69**, 034909 (2004).
[25] K. Aamodt *et al.* (The ALICE Collaboration), Phys. Rev. Lett. **106**, 032301 (2011).
[26] K. Aamodt *et al.* (ALICE Collaboration), Eur. Phys. J. C **68**, 89 (2010).
[27] T. Hirano, U. W. Heinz, D. Kharzeev, R. Lacey, and Y. Nara, Phys. Lett. B **636**, 299 (2006).
[28] T. Hirano, P. Huovinen, and Y. Nara (in preparation).
[29] J. Adams *et al.* (STAR Collaboration), Phys. Rev. C **72**, 014904 (2005).
[30] M. Luzum, Phys. Rev. C **83**, 044911 (2011).
[31] P. F. Kolb, Heavy Ion Phys. **15**, 279 (2002).
[32] F. Gelis, E. Iancu, J. Jalilian-Marian, and R. Venugopalan, Ann. Rev. Nucl. Part. Sci. **60**, 463 (2010).
[33] H. Song, S. A. Bass, U. W. Heinz, T. Hirano, and C. Shen, Phys. Rev. Lett. **106**, 192301 (2011).